

Full Waveform Inversion of the Kinematics of a Simulated Crack Inside an Artificial Rock

Albert C. To and Steven D. Glaser

Department of Civil and Environmental Engineering, University of California, Berkeley, U.S.A.

1 EXPERIMENTAL SETUP

In this paper, a full waveform inversion of the kinematics of a simulated crack inside an artificial rock plate is presented. To simulate a Mode I crack, a cylindrical piezoelectric (PZT) crystal of 13.45 mm diameter and 7.16 mm thickness was embedded inside a 850×850×42 mm³ gypsum plate, at a vertical distance of 15.7 mm from the top surface of the plate (Fig. 1). The piezoelectric crystal expands (or contracts) in the axial direction and contracts (or expands) in the radial direction due to the input of an electric signal (Fig. 2). The gypsum plate is made out of a ready-mix dry powder called Die-Keen from Modern Materials. Some physical properties of the plate are listed in Table 1.

Table 1 Physical Properties of the Gypsum Plate

Density (ρ)	2.6 g/cm ³
p-wave velocity (V_p)	4.23 mm/ μ s
s-wave velocity (V_s)	2.35 mm/ μ s
Q_p	70
Q_s	29

Three high-fidelity normal displacement sensors (Glaser et al., 1998) were placed on the top surface of the plate in a radial pattern, 45° apart from each other and at a radial distance of 70 mm from the source. The axial direction of the source lines up with Sensor 3. Each sensor has a flat response from 12 kHz to 1 MHz and was calibrated by a capillary break procedure developed by Breckenridge et al (1990). The transient responses due to the excitation of the source were digitally sampled at a 0.2 μ s interval at 14-bit resolution.

In each case, a single cycle sinusoidal wave having peak-to-peak voltage of about 600 V and bandpassed between 50 kHz and 20 MHz was used to excite the PZT crystal. The central frequencies of the first input signal and the second input signal are 400 kHz and 1 MHz, respectively, as shown in Figure 3. An example of the time-

displacement waveforms recorded due to the first and second input signals are shown in Figs 4 and 5, respectively.

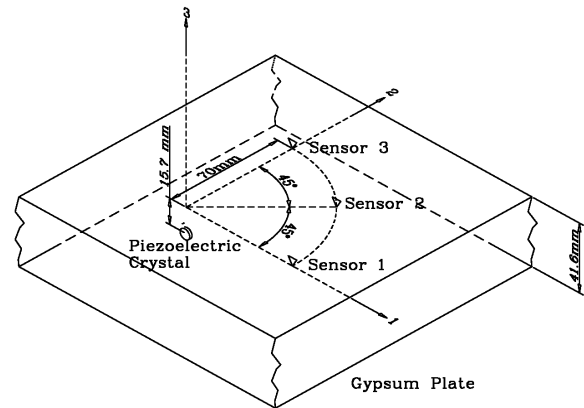


Figure 1 A Gypsum Plate with a Piezoelectric Crystal Embedded Inside and Sensors on the Top Surface

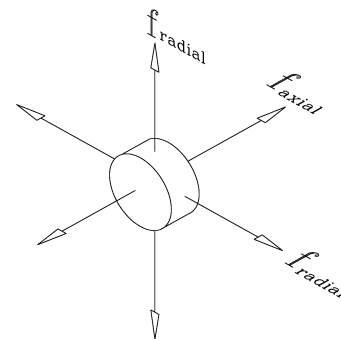


Figure 2 Kinematics of the Piezoelectric Crystal

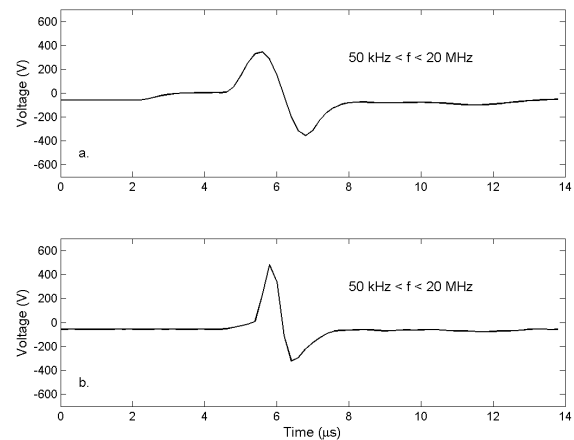


Figure 3 Input Electric Signals to the Piezoelectric Crystal with Various Central Frequencies: a) 400 kHz and b) 1 MHz.

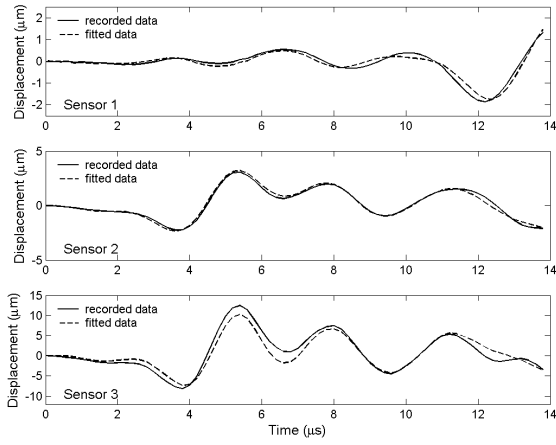


Figure 4 Comparison of Recorded Signals and Fitted Data for the Input Signal in Fig. 3a.

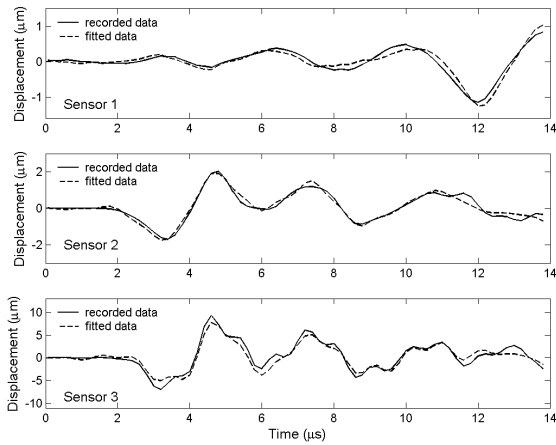


Figure 5 Comparison of Recorded Signals and Fitted Data for the Input Signal in Fig. 3b.

2 THEORETICAL FORMULATION

The kinematics of the simulated crack in the experiment can be described by linear combination of two force time functions, $f_{axial}(t)$ and $f_{radial}(t)$, in the axial and radial directions, respectively. The normal displacement time history $u(\mathbf{x}, t)$ at location \mathbf{x} due to $f_{axial}(t)$ and $f_{radial}(t)$ can be modeled as a convolution integral of the forces and the dynamic Green's functions:

$$u(\mathbf{x}, t) = G_{axial}(\mathbf{x}, t) * f_{axial}(t) + G_{radial}(\mathbf{x}, t) * f_{radial}(t) \quad (1)$$

where an asterisk denotes a convolution integral in the time variable. The Green's functions $G_{axial}(\mathbf{x}, t)$ and $G_{radial}(\mathbf{x}, t)$ are the respective normal displacements in the axial and radial directions at location \mathbf{x} and at time t due to a unit impulsive concentrated force at $t=0$. The Green's functions are calculated by the $f-k$ method (Kennett, 1983)

for an isotropic, homogeneous infinite plate with constant Q damping law (Kjartansson, 1979). The calculated Green's functions due to a localized force at $t=0 \mu s$ corresponding to each sensor are shown in Figs. 6 and 7 starting from $t=15 \mu s$ for clarity. With calculated Green's functions and recorded time-displacement signals from the three sensors, the force time functions in Eq. (1) are deconvolved in the time domain by least squares method (cf. Robinson and Treitel, 1980).

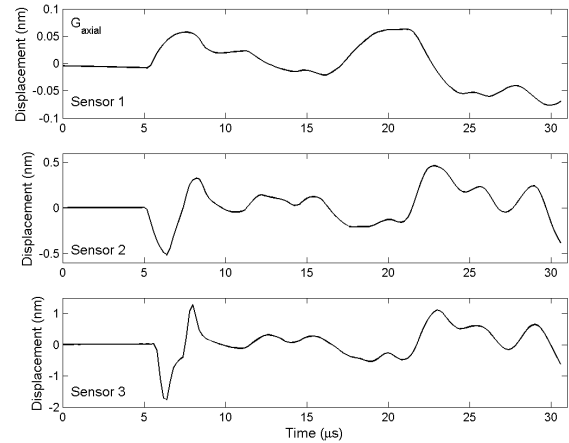


Figure 6 Green's Functions G_{axial} for Each Sensor

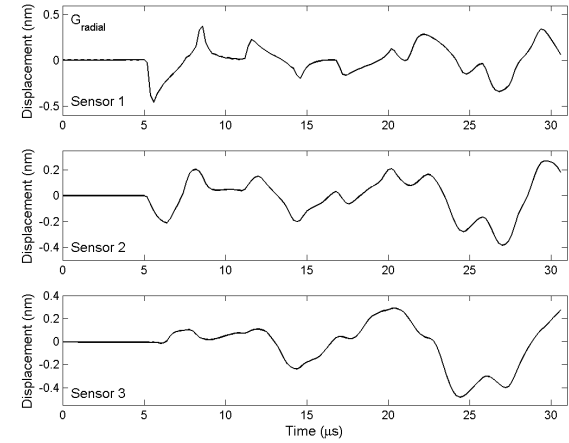


Figure 7 Green's Functions G_{radial} for Each Sensor

3 INVERSION RESULTS

After deconvolving the recorded acoustic emission signals with the corresponding Green's functions, the force time functions in Eq. (1) were estimated, and shown in Figs. 8-9 along with their Fourier spectra.

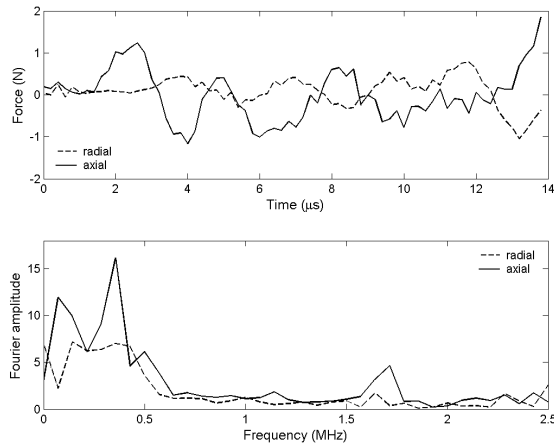


Figure 8 The Force Time Functions and Their Fourier Spectrum of the Simulated Crack Due to the Input Signal in Fig. 5a.

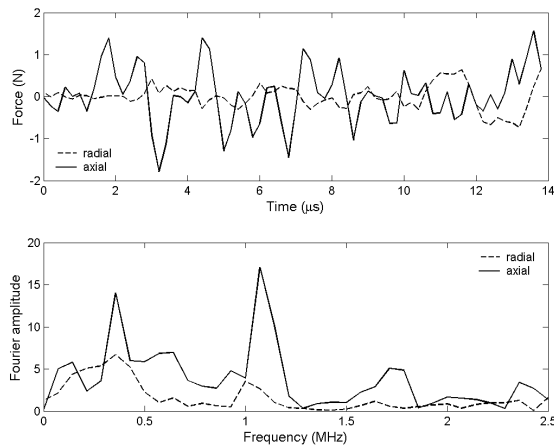


Figure 9 The Force Time Functions and Their Fourier Spectrum of the Simulated Crack Due to the Input Signal in Fig. 5b.

4. DISCUSSION

In each case, the force time functions $f_{axial}(t)$ and $f_{radial}(t)$ have opposite signs and thus obey the general mechanical behavior of the PZT crystal that the crystal contracts (or expands) in the radial direction when it expands (or contracts) in the axial direction. The waveform of the force time functions from 0 to 4 μs looks similar to their respective input electric signals in Fig. 3 while the later part of all the force time functions oscillates with varying amplitudes at different periods. In both cases, several peaks in the Fourier spectra are at the same frequencies: 0.36, 1.2 and 1.7 MHz. These results can be explained by the longitudinal modes of the PZT crystal, which are the solutions to the following equation:

$$\sin(f_n L/v)=0, \quad (2)$$

which have solutions:

$$f_n = nv/2L, \quad n=1,2,3,\dots \quad (3)$$

where f_n are the normal modes, L is the thickness of the PZT crystal and v is the longitudinal wave velocity:

$$v = \sqrt{\frac{E}{\rho}} \quad (4)$$

where E is Young's modulus. The first five modes are tabulated in Table 2 from solving Eq. (3) and from the Fourier spectra in Figs. 8-9. The first, fourth, and fifth modes match well with the peaks in the Fourier spectra of both cases (Figs. 8 and 9) while the second and third modes are identifiable in the second case only. Also, since the frequency content of the electric input signal is higher in the second case, the higher modes are excited more in the second case than in the first case.

Table 2. Longitudinal Normal Modes of the PZT Crystal (in MHz)

	n=1	n=2	n=3	n=4	n=5
From Normal Mode Theory	0.32	0.63	0.95	1.3	1.6
From Experiment	0.36	0.64	0.95	1.2	1.7

The fitted data in Figs. 4 and 5 are obtained by convolving the Green's functions with the force time function through Eq. (2). In each case, the fitted data has excellent match with the original recorded data.

REFERENCES

- Aki, K. and Richards, P. G., (2002). *Quantitative Seismology, Theory and Method*. University Science Books, Sausalito, CA.
- Breckenridge, F.R., Proctor, T.M., Hsu, N.N., Fick, S.E., and Eitzen, D.G. (1990). "Transient sources for acoustic emission work" in *Progress in Acoustic Emission, V, Proc. 10th International Acoustic Emission Symposium*, edited by K. Yamagushi, H. Takakashi, and H. Niitsuma (Japanese Society for Non-Destructive Inspection, Tokyo), 20-37.
- Glaser, S.D., Weiss, G., and Johnson, L.R. (1998). "Body waves recorded inside an elastic half space by an embedded, wideband velocity sensor" *J. Acoust. Soc. Am.*, 104, 1404-1412.
- Kennett, B. L. N., (1983). *Seismic Wave Propagation in Stratified Media*. Cambridge University Press.
- Robinson, E. A., and Treitel, S., (1980). *Geophysical Signal Analysis*. Prentice Hall, Englewood Cliffs, NJ.